



MR Imaging with Metal-suppression Sequences for Evaluation of Total Joint Arthroplasty¹

Brett S. Talbot, MD
Eric P. Weinberg, MD

Abbreviations: ALVAL = aseptic lymphocyte-dominated vasculitis-associated lesion, MARS = metal artifact reduction sequence, MAVRIC = multiacquisition with variable-resonance image combination, SAR = specific absorption rate, SEMAC = slice encoding for metal artifact correction, SNR = signal-to-noise ratio, STIR = short inversion time inversion-recovery, VAT = view-angle tilting

RadioGraphics 2016; 36:209–225

Published online 10.1148/rg.2016150075

Content Codes:   

¹From the School of Medicine and Dentistry, University of Rochester Medical Center—University Medical Imaging, 601 Elmwood Ave, Box 648, Rochester, NY 14642. Presented as an education exhibit at the 2014 RSNA Annual Meeting. Received March 21, 2015; revision requested June 30 and received August 26; accepted September 18. For this journal-based SA-CME activity, the authors, editor, and reviewers have disclosed no relevant relationships. **Address correspondence** to B.S.T. (e-mail: Brett_Talbot@urmc.rochester.edu).

©RSNA, 2015

SA-CME LEARNING OBJECTIVES

After completing this journal-based SA-CME activity, participants will be able to:

- List common artifacts associated with metallic hardware at MR imaging, as well as the parameters that should be optimized for metallic artifact reduction.
- Describe the currently available metal-suppression sequences for MR imaging.
- Identify the appearance of common complications of total joint arthroplasty at MR imaging with metal-suppression sequences.

See www.rsna.org/education/search/RG.

Metallic artifact at orthopedic magnetic resonance (MR) imaging continues to be an important problem, particularly in the realm of total joint arthroplasty. Complications often follow total joint arthroplasty and can be expected for a small percentage of all implanted devices. Postoperative complications involve not only osseous structures but also adjacent soft tissues—a highly problematic area at MR imaging because of artifacts from metallic prostheses. Without special considerations, susceptibility artifacts from ferromagnetic implants can unacceptably degrade image quality. Common artifacts include in-plane distortions (signal loss and signal pileup), poor or absent fat suppression, geometric distortion, and through-section distortion. Basic methods to reduce metallic artifacts include use of spin-echo or fast spin-echo sequences with long echo train lengths, short inversion time inversion-recovery (STIR) sequences for fat suppression, a high bandwidth, thin section selection, and an increased matrix. With care and attention to the alloy type (eg, titanium, cobalt-chromium, stainless steel), orientation of the implant, and magnetic field strength, as well as use of proprietary and nonproprietary metal-suppression techniques, previously nondiagnostic studies can yield key diagnostic information. Specifically, sequences such as the metal artifact reduction sequence (MARS), WARP (Siemens Healthcare, Munich, Germany), slice encoding for metal artifact correction (SEMAC), and multiacquisition with variable-resonance image combination (MAVRIC) can be optimized to reveal pathologic conditions previously hidden by periprosthetic artifacts. Complications of total joint arthroplasty that can be evaluated by using MR imaging with metal-suppression sequences include pseudotumoral conditions such as metallosis and particle disease, infection, aseptic prosthesis loosening, tendon injury, and muscle injury.

©RSNA, 2015 • radiographics.rsna.org

Introduction

Performing a magnetic resonance (MR) imaging examination in a patient with an implanted metal device has in the past resulted in poor-quality images. As a result, these examinations were avoided. However, there exists a need to examine patients who have implanted metal devices. In particular, orthopedic surgeons require imaging studies in patients with joint replacements for a range of different problems and pathologic conditions. In the United States, the number of joint replacements has increased; 332,000 total hip replacements and 719,000 total knee replacements were performed

TEACHING POINTS

- The first integrated approach to a metal-suppression sequence was described by Olsen et al and is referred to as the metal artifact reduction sequence (MARS). In its original formulation, this sequence utilized an increased section-select and radiofrequency bandwidth, thin section selection (3–4 mm), an increased echo train length, decreased echo spacing, and an increased image matrix.
- Classified as a multispectral technique, SEMAC is a powerful tool to reduce through-section distortion. At its core, SEMAC is a two-dimensional fast spin-echo or turbo spin-echo sequence in which each section is phase encoded in the third dimension. This third dimension, or Z-phase encoding, from all of the overlapping sections gives a detailed map of exactly how magnetic susceptibility has distorted the image.
- MAVRIC is a spin-echo–based sequence that uses a series of frequency-selective excitations, multidirectional VAT, computational postprocessing, and a standard three-dimensional readout.
- The hallmark appearance of metallosis at MR imaging is a lobular mass adjacent to the joint capsule or bone that shows homogeneous low signal intensity on T2-weighted images and is surrounded by a well-demarcated rim with low T2 signal intensity. On T1-weighted images, the mass shows intermediate-to-high signal intensity, with focal areas of low T1 signal intensity typically at the periphery.
- Hallmark imaging features of particle disease at T2-weighted MR imaging are fluid collections or effusions with intermediate-to-high signal intensity and segmental or irregular foci with low signal intensity at the periphery that represent disorganized and irregular synovitis.

in 2010 (1). Simultaneously, there is a trend toward joint replacement occurring in younger, more active patients. The average age for knee replacement decreased from 68 years in 2000 to 66 years in 2009 (2). These joint replacements have a limited life span, resulting in a need for revision arthroplasty in the future. Orthopedic surgeons and their patients have also had to contend with ongoing manufacturer recalls of certain joint replacement models. In these patients, imaging is often required to determine the proper course of action.

There is an ongoing and increasing need for optimal imaging evaluation in patients with joint replacements. Advances in MR imaging hardware and software now allow significantly improved image quality in the presence of ferromagnetic materials. MR imaging of joint replacements is now an effective method for evaluating complications of joint arthroplasty. MR imaging of metal, and specifically that involved in joint arthroplasty, is continuing to evolve as new hardware and new pulse sequences are released. Musculoskeletal radiologists will need to stay current with the latest developments in the field so that the quality and diagnostic utility of our images can continue to improve for the benefit of patients and referring clinicians.

Magnetic Fields and Metals

Various forces affect the local magnetic field and generate MR imaging artifacts (Fig 1). In general, these forces can be separated into diamagnetic, paramagnetic, and ferromagnetic effects (3). Objects or substances with diamagnetic properties exhibit no intrinsic magnetic moment. Diamagnetism exerts a small repulsive effect on the local magnetic field. Materials such as soft tissue, water, copper, and nitrogen demonstrate diamagnetism. On a gross scale, the human body can be thought of as a giant diamagnetic interferent. Paramagnetism has a relatively small attractive effect on the local magnetic field, and paramagnetic substances have a positive magnetic moment. Materials such as iron ions (hemoglobin breakdown products), oxygen, magnesium, and gadolinium have paramagnetic effects. This is the primary effect used with gadolinium-based contrast agents (4). Ferromagnetic substances demonstrate a positive magnetic moment, but, in contrast to paramagnetic and diamagnetic materials, they have a strong positive (attractive) magnetic susceptibility. Examples include solid iron and iron alloys (eg, stainless steel), cobalt, and nickel. Ferromagnetic effects are the primary drivers of metal-related artifacts at MR imaging.

In modern clinical MR imaging magnets, the B_0 field is typically homogeneous to within a few parts per million (ppm), with 1 ppm equal to approximately 60 Hz at 1.5 T. Common orthopedic metallic implants introduce field heterogeneity by means of predominantly ferromagnetic effects, largely in the frequency-encoding and section-selection directions. Three of the most common arthroplasty formulations and alloys perturb the local field to varying degrees, with titanium producing the least susceptibility and stainless steel producing the greatest susceptibility (Table 1) (5).

One important principle is that the magnitude of ferromagnetic susceptibility increases in a linear relationship with B_0 . Therefore, the overall degree of artifact is substantially lower at 1.5 T than at 3.0 T. The improved signal and image quality afforded by a new 3.0-T magnet may produce images laden with so much metallic artifact that the examination may be of no clinical utility.

Artifacts Due to Metallic Implants

Specific artifacts that can be attributed to metallic implants have been discussed and characterized by several investigators (6,7). The most common and troublesome artifacts and their associated reduction methods are briefly summarized in Table 2.

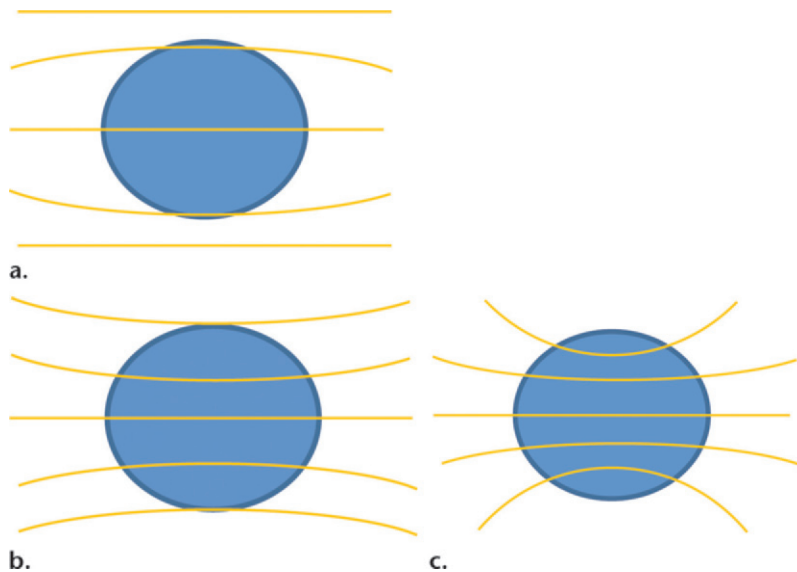


Figure 1. Magnetic fields and tissue-metal interactions. **(a)** Diamagnetic materials have no intrinsic magnetic moment and a small repulsive effect on the local field. Materials such as tissue, water, copper, and nitrogen have diamagnetic interactions. The human body can be thought of as a giant diamagnetic interferent. **(b)** Paramagnetic materials have a positive magnetic moment and a small attractive effect on the local field. Materials such as oxygen, iron ions, magnesium, and gadolinium have primarily paramagnetic properties. This is the primary effect used in gadolinium-based contrast enhancement (increased T1 and T2 relaxation times). **(c)** Ferromagnetic materials have a positive magnetic moment and a strong positive (attractive) magnetic susceptibility. Materials such as iron, cobalt, and nickel have ferromagnetic properties. This is the primary driver of metal artifact at MR imaging.

Table 1: Susceptibility of Common Prosthetic Implant Materials

Metal or Alloy	Susceptibility at 1.5 T (ppm)
Titanium	180
Cobalt-chromium	900
Stainless steel	3000–5000

In-Plane Distortions (Signal Loss and Pileup Artifacts)

Perhaps the most troublesome source of metal-associated artifacts can be characterized within the broad category of in-plane distortions. Primary among in-plane distortions are signal loss and pileup artifacts (7). These distortions arise from local field inhomogeneities instigated by the ferromagnetic properties of the implant material. Signal loss, a characteristic cloud of low signal intensity surrounding a metallic prosthesis, is mediated by T2* dephasing. To reduce and mitigate this phenomenon, the use of spin-echo, fast spin-echo, or turbo spin-echo sequences is recommended. Spin-echo-based sequences use multiple radiofrequency pulses to refocus and reduce the degree of T2* decay, thus mitigating and reducing signal loss. The use of short echo spacing and an intermediate-to-long echo train length

further reduces signal loss artifact (5). Gradient-echo-based sequences should be avoided, as such parameters fundamentally amplify the degree of T2* decay, leading to substantial signal loss.

An additional problem-solving technique includes swapping the phase- and frequency-encoding directions. Metal-related artifact tends to be least prominent when the lengthiest portion of the prosthesis is aligned parallel to the B_0 field. Swapping the phase- and frequency-encoding directions may change the orientation of in-plane artifacts or reveal key anatomic structures near curved or curvilinear portions of a prosthesis. This strategy rarely eliminates artifacts but may shift signal loss or pileup artifacts to less anatomically important locations.

Poor or Absent Fat Suppression

Spectral-based fat suppression is unlikely to be of benefit around metallic prostheses (5). This concept is once again rooted in the ferromagnetic properties of the implant. For successful spectral fat saturation, the local B_0 must be as homogeneous as possible to take advantage of the relatively small differences in the chemical shifts of fat and water. The ferromagnetic properties of the implant cause marked variability in the local field, and this perturbation of local field homogeneity leads to incomplete or absent fat suppression.

Table 2: Common Metal-associated Artifacts and Reduction Methods

Artifact	Reduction Methods
In-plane distortion (pileup and signal loss)	High bandwidth, swap frequency and phase, VAT
Signal loss (T2* dephasing)	Spin-echo or fast spin-echo sequences (avoid gradient-echo sequences)
Poor or absent fat suppression	STIR sequences or Dixon-based techniques (avoid spectral-selective fat-suppression methods)
Geometric distortion	High readout bandwidth
Through-section distortion	Thin section selection, SEMAC and MAVRIC sequences

Note.—MAVRIC = multiacquisition with variable-resonance image combination, SEMAC = slice encoding for metal artifact correction, STIR = short inversion time inversion-recovery, VAT = view-angle tilting.

A more tenable alternative method is the STIR technique. At its base, STIR relies on the difference in T1 relaxation times of fat and water and is independent of their chemical shift. Similarly, Dixon-based techniques may allow adequate fat suppression around metal. In clinical practice, STIR has proven to be the most robust technique and is our preferred method of fat suppression around metallic implants.

Geometric Distortion

The different resonant frequencies of metal or metal alloy and the surrounding tissue cause geometric distortion artifact in a way akin to that in which chemical shift artifact is produced. This cohabitation of metal or metal alloy within the same voxel as the tissue of interest leads to the spreading out of the pixels over a larger range, creating a distorted image. This is most often rectified by increasing the receiver bandwidth. In essence, increasing the bandwidth will limit the spread of geometric distortion and confine it to a smaller pixel range. The obvious trade-off with this technique is a decreased signal-to-noise ratio (SNR). A balance should be sought in which distortion is limited but signal is maintained at diagnostic levels. Because bandwidth varies among vendors and institutions, no specific bandwidth values are recommended.

Through-Section Distortion

The majority of conventional metal artifact reduction strategies affect in-plane artifacts. Abnormalities that violate boundaries between sections can be particularly troublesome. Among traditional methods to reduce such anomalies is the use of thinner sections. By obtaining a thinner section, the partial volume effects and diminished SNR of through-plane distortion can be remedied. Almost paradoxically, the SNR can be improved near the prosthesis in the region of through-section distortion by using a thinner

section. However, the SNR outside of the region of through-section artifact (the majority of the image) will be decreased.

One additional strategy for metal artifact reduction is to increase the resolution (matrix). Although this approach can provide a further reduction of in-plane artifacts, such improvements are typically at the fringe of diminishing returns. Increased resolution often affords the smallest reduction in metal artifact compared with other available methods. This reduction of in-plane artifact comes at the expense of further reduction in the SNR and increased imaging time because of the increased number of phase-encoding steps.

Several of the strategies previously described, including increasing the bandwidth, decreasing the section thickness, and increasing the resolution, will tend to reduce the SNR. The most effective strategy for gaining back some lost SNR is to increase the number of signals acquired (number of excitations), which will, unfortunately, increase the imaging time.

Advanced Metal-suppression Packages and Sequences

The first integrated approach to a metal-suppression sequence was described by Olsen et al (8) and is referred to as the metal artifact reduction sequence (MARS). In its original formulation, this sequence used an increased section-select and radiofrequency bandwidth, thin section selection (3–4 mm), an increased echo train length, decreased echo spacing, and an increased image matrix. This sequence is widely available on most clinical MR imaging systems.

Notably, the term MARS can be used in proprietary nomenclature to refer to a specific pulse sequence or package but may alternatively be used in reference to the concept of metal suppression in general. Because of this ambiguity, not all sequences labeled “MARS” use the same set of parameters. Close scrutiny of any sequence

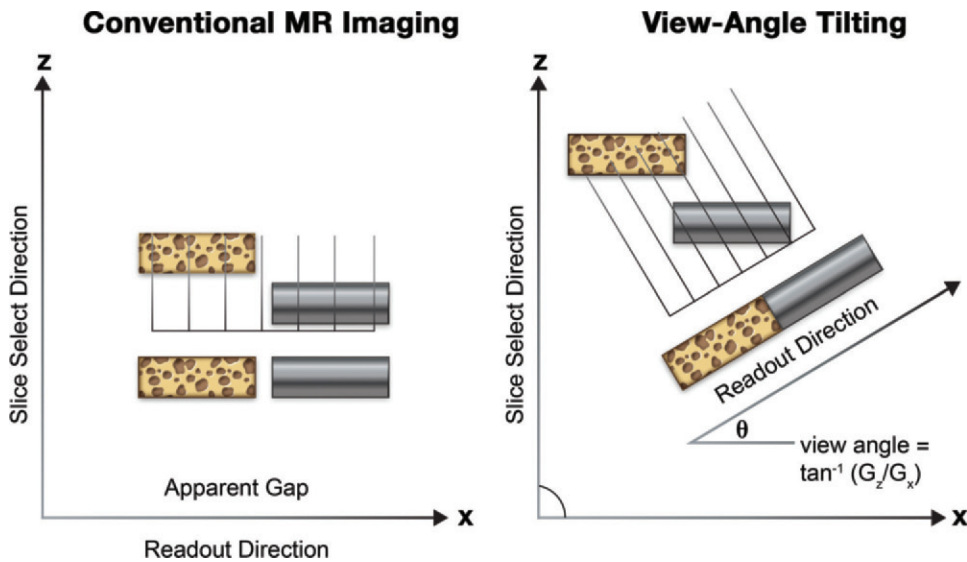


Figure 2. VAT. VAT minimizes in-plane distortions by the addition of an altered readout gradient, given as the angle θ (right graph). This will primarily reduce signal loss and pileup artifacts, with the trade-off of a small degree of blurring. Note the apparent gap between the bone (speckled) and the metal (gray) in the graph on the left. After application of VAT, the apparent gap is reduced. VAT is a key component of WARP and some proprietary MARS sequences. G_x = reading gradient, G_z = concentration gradient, \tan = tangent.

Table 3: Typical MARS Protocol

Sequence	Echo Time (msec)	Repetition Time (msec)	Section Thickness (mm)	Frequency \times Phase	Echo Train Length	Bandwidth (kHz)	Frequency Direction
STIR (coronal)	18	3200	3	256 \times 192	12	50	SI
T2-weighted (axial)	50	4000	4	384 \times 224	16	100	AP
T1-weighted (axial)	15	850	4	384 \times 224	16	100	AP
Proton-density-weighted (coronal)	17	2375	3	320 \times 224	10	100	SI

Note.—We use this protocol on a 1.5-T GE Healthcare (Milwaukee, Wis) MR imaging unit. AP = anteroposterior, SI = superoinferior.

or package labeled as “MARS” is therefore recommended. In our practice, we use a nonproprietary MARS package at 1.5 T. Our current imaging parameters are listed in Table 3.

Other more advanced methods for metal artifact suppression have recently transitioned from the research realm into everyday clinical practice. Foremost among these are the WARP (Siemens Healthcare, Munich, Germany), SEMAC, and MAVRIC sequences.

WARP

The premise of WARP is to optimize the standard principles of MARS and to include multidirectional VAT to further reduce in-plane distortion (9). VAT was initially described by Cho et al (10) and is now a classic and commonly used strategy

to reduce in-plane artifacts. An additional gradient is applied during signal readout along the section-select direction. This gradient results in a shearing effect on the pixels of interest. This results in a section that can be viewed as if on a slight angle or tilt. The VAT gradient is equal to the excitation and cancels any off-resonance effects. This concept is shown in Figure 2. One major drawback of VAT is the addition of a small degree of blurring. VAT is unable to correct for through-section distortions.

WARP represents a proprietary package rather than a specific technique, and, in future iterations, it will likely be combined with other multispectral imaging techniques. In our practice, we use WARP with a 3.0-T Siemens magnet at an outpatient imaging center. Our current imaging parameters are listed in Table 4.

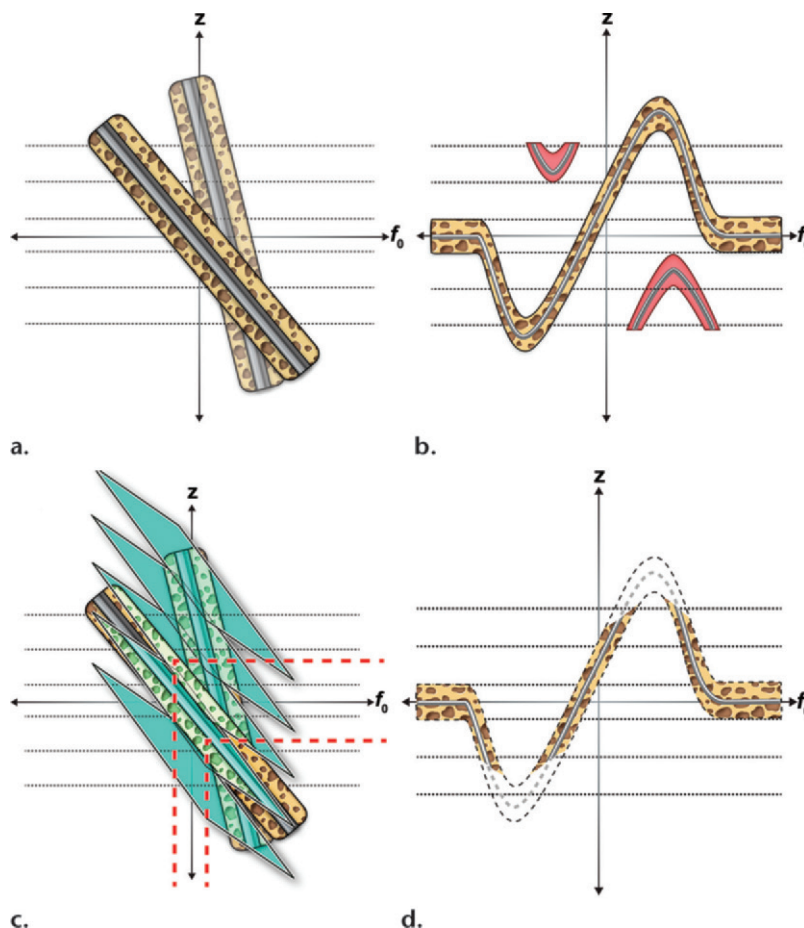


Figure 3. SEMAC process. (a) Excitation: Equal section-selection gradients are applied to the region of interest. The excited area is depicted as bone (speckled) with a metal prosthesis (gray) in a–d. (b) Section distortion: Ferromagnetic effects lead to a series of distorted sections, one of which is shown here. With large frequency offsets, the distorted area may extend outside the encoded field of view (red areas). (c) Profile resolution: Individual section profiles are then resolved with additional Z-phase encoding (green rhombi). A specific section is sampled and is reconstructed in a pixel-by-pixel fashion. (d) Reconstruction: Regions of high distortion are suppressed and essentially “taper.” After multiple distorted sections are mapped, the signals from different excited sections are combined, and through-plane distortions are corrected. (Figure 3 adapted, with permission, from reference 12.)

Table 4: Standard WARP Protocol

Sequence	Echo Time (msec)	Repetition Time (msec)	Section Thickness (mm)	Frequency × Phase	Echo Train Length	Bandwidth (Hz/pixel)	Frequency Direction
STIR (coronal)	54	3000	3	320 × 240	22	504	SI
T2-weighted (axial)	38	3040	3	320 × 256	24	395	AP
T1-weighted (axial)	7	500–800	4	320 × 256	24	401	AP
Proton-density-weighted (coronal)	20	2000	3	320 × 240	14	401	AP

Note.—We use WARP on a 3.0-T Siemens Healthcare MR imager. AP = anteroposterior, SI = superoinferior.

SEMAC

Classified as a multispectral technique, SEMAC is a powerful tool to reduce through-section distortion (11). At its core, SEMAC is a two-dimensional fast spin-echo or turbo spin-echo sequence in which each section is phase encoded in the third dimension. This third dimension, or Z-phase encoding, from all of the overlapping sections gives a detailed map of exactly how magnetic susceptibility has distorted the image. Complex reconstruction algorithms are then used

to correct these through-section distortions and shift them to their proper positions within the final image. This process is depicted in Figure 3. The primary drawback of SEMAC is the requisite increase in imaging time.

MAVRIC

A second multispectral technique, MAVRIC, is able to address both through-section and in-plane artifacts (13). Some large specialty hospitals use this technique and have demonstrated its efficacy

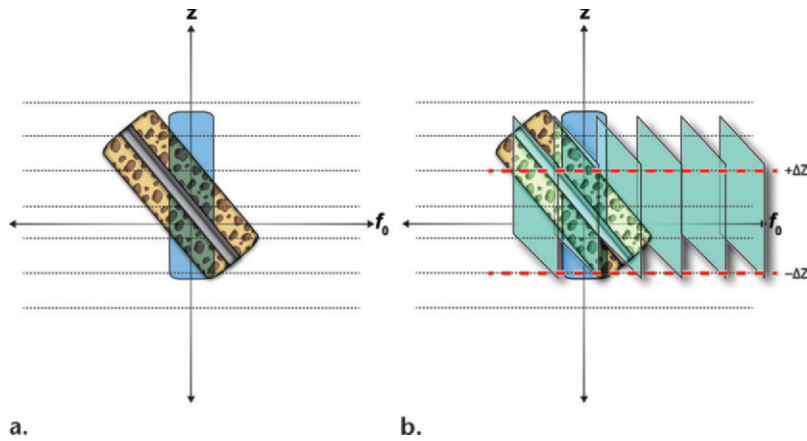


Figure 4. MAVRIC process. (a) The sequence begins with frequency-selective excitation and refocusing. A representative bone (speckled) with a central metal rod (gray) is shown. A region of interest is excited across the frequency range (blue rectangle in a and b). (b) Subsequently, three-dimensional fast spin-echo imaging is used to obtain the range of excited frequencies over the given region. Many section-encoding steps may be required to cover the entire field of view (green rhombi in b). (Adapted, with permission, from reference 12.)

Table 5: Common Metal-suppression Sequences

Sequence or Package	Availability	Basic Physics or Principles of Protocol
MARS	Most clinical magnets	High-bandwidth sequences (T1-weighted, T2-weighted, STIR, proton-density-weighted); some proprietary MARS sequences include VAT
WARP	Siemens Healthcare magnets	High-bandwidth MARS with multidirectional VAT
SEMAC	Siemens Healthcare magnets	Backfolding of off-resonance signal
MAVRIC	GE Healthcare magnets	Spatially nonselective excitation and refocusing with VAT and proprietary antiblurring algorithm

(14). MAVRIC is a spin-echo-based sequence that uses a series of frequency-selective excitations, multidirectional VAT, computational postprocessing, and a standard three-dimensional readout. To begin, a frequency-selective excitation and refocusing are applied to interrogate and map a specific range of frequencies over the field of interest. Because the range of frequencies may be relatively small compared with the interrogated anatomy, many section-encoding steps may be required to cover the entire field of view. Multidirectional VAT is applied to further reduce any in-plane artifacts in a manner similar to its use in WARP. At readout, a number of proprietary smoothing and antiblurring algorithms are applied. This results in a dramatic reduction in metallic artifact. The basic physics principles behind MAVRIC are shown in Figure 4. The two primary trade-offs are increased imaging time and increased specific absorption rate (SAR). Because of SAR requirements, MAVRIC is more successful at 1.0 T or 1.5 T (as discussed in the next section).

Further extensions of these concepts include MAVRIC-SEMAC hybrids (15), off-resonance suppression (12), and other hybridized approaches. These techniques appear promising and may soon be available in general clinical practice. Common metal-suppression sequences are summarized in Table 5.

Field Strength and Specific Issues at 3.0 T

The SAR is related to many imaging parameters but is most closely aligned with the radiofrequency bandwidth, B_0^2 , and the square of the flip angle. The foundation of good metal suppression is high-bandwidth imaging, a prolonged echo train length, and a large number of signals acquired, making SAR an important concern in metal-suppression imaging. Although these factors may not lead to SAR time-out at 1.0 T or 1.5 T, care must be taken at higher field strengths to ensure that the entire protocol can be performed. For nonmultispectral metal-suppression techniques such as MARS and WARP, SAR time-out is uncommon. However, the increased number of signals acquired and additional section-selection steps in MAVRIC and SEMAC have the potential to lead to SAR time-out.

Some authors suggest that the SAR may be overestimated on clinical magnets because much of the basic physics behind SAR calculations tends to overestimate the effect. As a further illustration, Koff et al (14) and Tayton et al (16) point out that the risk of in vivo damage from MR imaging-related heat deposition is overestimated by comparing it to the heat deposition of cemented prostheses. They note that the exothermic reaction of methyl methacrylate cement polymerization

generates 50°–70°C in vitro and up to 48°C in vivo. This degree of heat deposition is several-fold higher than heat deposition from MR imaging, even at 3.0 T. Thus, by comparison, the degree of SAR-related heating may not be clinically evident or relevant.

Of note, few joint prostheses bear the U.S. Food and Drug Administration label of “MR safe” or “MR conditional.” Therefore, the majority of MR imaging of joint arthroplasty implants is performed in an off-label fashion. It is the responsibility of the radiologist to ensure patient safety (14).

Special considerations are required when using T1-weighted sequences in metal suppression. As discussed earlier, short echo spacing is required for good metal suppression. Short echo spacing is difficult to achieve with T1-weighted imaging, leading to poorer metal suppression. In addition, the low repetition times required for T1-weighted sequences often lead to a substantial increase in SAR at 3.0 T secondary to the increased imaging time. For these reasons, T1-weighted sequences are used less frequently.

Few studies have published data on the utility of SEMAC at a field strength of 3.0 T. In the region of the spine, SEMAC appears efficacious in reducing artifact compared with standard two-dimensional fast spin-echo sequences. One investigation (17) was successful in showing an enhanced degree of detail of the bone-metal interface, improved prosthetic detail, and better delineation of the vertebral bodies, dural sac, and neural foramina.

Complications of Total Joint Arthroplasty

A variety of pathologic conditions associated with joint arthroplasty can be evaluated with use of metal-suppression MR imaging sequences (Table 6).

Because of its availability and cost, some have questioned if computed tomography (CT) could replace MARS MR imaging, particularly for evaluation of the hip (18). It appears that CT may be superior to MARS MR imaging for evaluation of the bone-metal interface and detection of osteolysis; however, CT continues to be less useful for evaluating pseudotumoral conditions and detecting pathologic muscle conditions. Other investigators (19) have compared the utility of MARS MR imaging and ultrasonography (US) for evaluation of painful hip arthroplasty. They suggest that MARS MR imaging is superior to US for detection of pseudotumoral conditions and pathologic muscle conditions, while US is superior for evaluation of joint effusion and pathologic tendon conditions. It is reasonable to assume that more contemporary methods of

Table 6: Common Complications of Total Joint Arthroplasty Assessed at Metal-suppressed MR Imaging

Metallosis
Particle disease
Infection
Loosening
Tendon injury
Muscle injury

metal suppression (WARP, MAVRIC, SEMAC) will outperform MARS, particularly at the bone-metal interface. This ability to show improved detail at the bone-metal interface and greater muscular detail will allow modern MR imaging to likely outperform CT and US for evaluation of these indications.

Pseudotumoral Conditions

Metallosis

The nomenclature surrounding this condition varies according to source and is not uniform in the literature or in all practices (20,21). The preferred terminology in our practice is *adverse reaction to metallic debris* or simply *metallosis*. The formal term associated with this disease process in the pathology literature is *aseptic lymphocyte-dominated vasculitis-associated lesion (ALVAL)*—a histopathologic diagnosis. Because of this lack of clarity in nomenclature, radiologists and orthopedists alike may, often erroneously, refer to any metal-associated pseudotumor or collection in metal-on-metal arthroplasty as an ALVAL (22).

The hallmark appearance of metallosis at MR imaging is a lobular mass adjacent to the joint capsule or bone that shows homogeneous low signal intensity on T2-weighted images and is surrounded by a well-demarcated rim with low T2 signal intensity. On T1-weighted images, the mass shows intermediate-to-high signal intensity, with focal areas of low T1 signal intensity typically at the periphery (Fig 5). Grading systems have been established in the literature (23). Although the degree of clinical symptoms appears to be independent of the imaging findings (24), some investigators (25) have established that MR imaging findings can be correlated with the severity of ALVALs.

In patients with cobalt-chromium-based metal-on-metal arthroplasty alloys, a number of studies (26,27) indicate that the degree of metal-on-metal wear can be evaluated by measuring serum chromium and cobalt concentrations. Serum chromium levels greater than 17 µg/L and serum cobalt levels greater than 19 µg/L



Figure 5. Metallosis in a 61-year-old woman after metal-on-metal right hip total arthroplasty. The patient’s blood levels of cobalt and chromium were elevated; joint fluid metal levels were not obtained. (a, b) Axial T2-weighted (a) and proton-density-weighted (b) 3.0-T WARP MR images show a polylobulated fluid collection (arrows) adjacent to the greater trochanter. The collection shows homogeneous low signal intensity in a and intermediate signal intensity in b, with small low-signal-intensity foci seen at the periphery in b. The halo of susceptibility artifact is greatly reduced by using WARP, enabling visualization and characterization of the fluid collection and its communication with the greater trochanter and the arthroplasty hardware (arrowhead in b). (c) Radiograph shows the outline of the fluid collection (arrow) but does not clearly show its communication with the greater trochanter or the arthroplasty hardware.

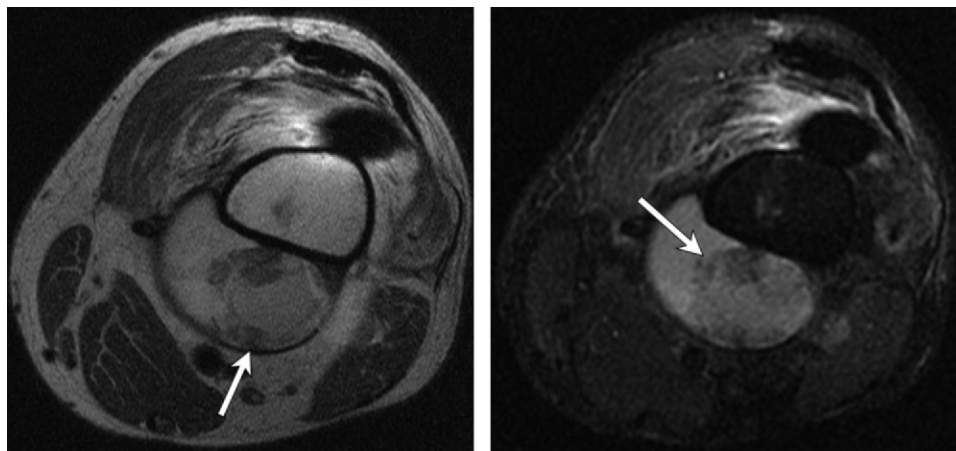
appear to be associated with metallosis and are at least 10-fold higher than in patients without metallosis. There is some indication that joint fluid aspirate levels of cobalt and chromium may also correlate with the degree of tissue degradation observed during explant or revision surgery. However, the range of chromium and cobalt levels in joint fluid aspirate varies widely (28). Unfortunately, to our knowledge, it appears that no large-scale evaluation of cobalt and chromium levels obtained from joint fluid aspirate

in asymptomatic patients has been performed. Therefore, the exact utility of joint fluid aspirate for metallosis evaluation remains unclear.

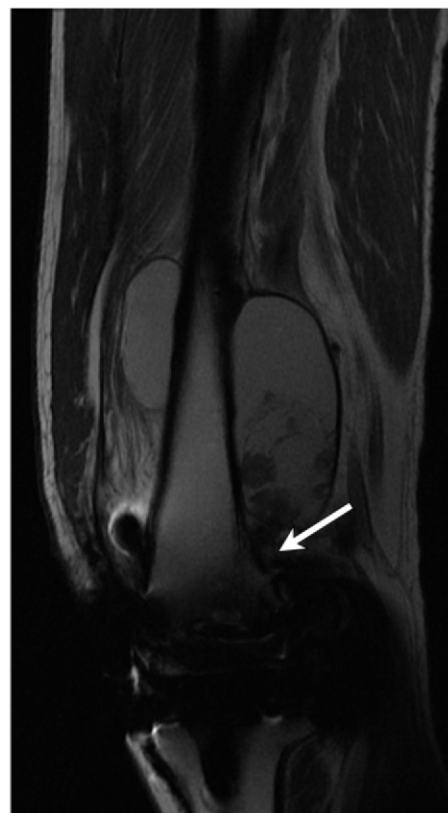
Particle Disease

Failure of implanted metallic prostheses can be related to particle disease (29). This heterogeneous group of pathologic conditions refers to the body’s response to microscopic particles of high-molecular-weight polyethylene (from the arthroplasty device liner material), cement, or metal that can be shed from the implant into the surrounding tissues. Unlike metallosis, which is caused by a classic hapten-mediated type IV hypersensitivity reaction, particle disease stimulates macrophages, which in turn may lead to inflammatory synovitis and osteoclast activation (30). This may lead to clinically important osteolysis, fluid collections, and arthroplasty implant failure. A number of inflammatory cytokines are implicated in this process.

Hallmark imaging features of particle disease at T2-weighted MR imaging are fluid collections or effusions with intermediate-to-high signal intensity, with segmental or irregular low-signal-intensity foci at the periphery that represent



a. **b.**
Figure 6. Particle disease in a 64-year-old man after left knee total arthroplasty. **(a, b)** Axial T2-weighted **(a)** and STIR **(b)** MARS MR images show a multiloculated, complex, predominantly high-signal-intensity fluid collection. Scattered internal foci with heterogeneous low signal intensity (arrow) are seen along the posteromedial aspect of the distal part of the femur, deep to the vastus medialis. **(c)** Sagittal T2-weighted MARS MR image enables visualization of the inferior margin of the collection, which extends to the femoral prosthesis. The small region of cortical thinning and high T2 signal intensity (arrow) near the prosthesis represents subtle osteolysis.



c.

disorganized and irregular synovitis. (Fig 6). The irregular peripheral low signal intensity helps solidify the diagnosis of particle disease because infection and osseous neoplasms are not likely to have peripheral low signal intensity and are much more likely to have high signal intensity at T2-weighted imaging. On T1-weighted images, zones of osteolysis can be seen as areas of intermediate signal intensity, again often with a peripheral low-signal-intensity rim. Early signs of particle disease include small effusions and irregular synovitis, which may be clinically silent (31). Subsequently, osteolysis may develop as regions of cortical thinning or expansile cortical disruption. The affected region may be somewhat removed from the arthroplasty articulation, as the inflammatory process can develop anywhere that particulate may locally migrate.

Infection

Infection is a known complication of total joint arthroplasty and is reported to occur in varying degrees in the literature. As many as 2%–3% of hip arthroplasties may be complicated by infection, with similar rates observed in other joints. The rate of infection may be higher in certain subpopulations of patients (32). Joint fluid aspiration with fluid culture remains the standard for diagnosis; however, false-positive and false-neg-

ative results complicate this method of analysis. The MR imaging appearance of infection can vary but is typified by an ill-defined pattern of soft-tissue edema, variable degrees of abscess formation or fluid collection, draining sinuses, joint effusion, marrow edema, periosteal reaction, and osseous destruction (Figs 7, 8). Peripheral, localized, or even diffuse enhancement can be seen after gadolinium-based contrast agent administration. A frequent finding is laminated synovial reaction or proliferation (29). The findings of infection can be contrasted with those of noninfected effusions, which typically lack associated marrow and soft-tissue edema (Fig 9). Clinically,

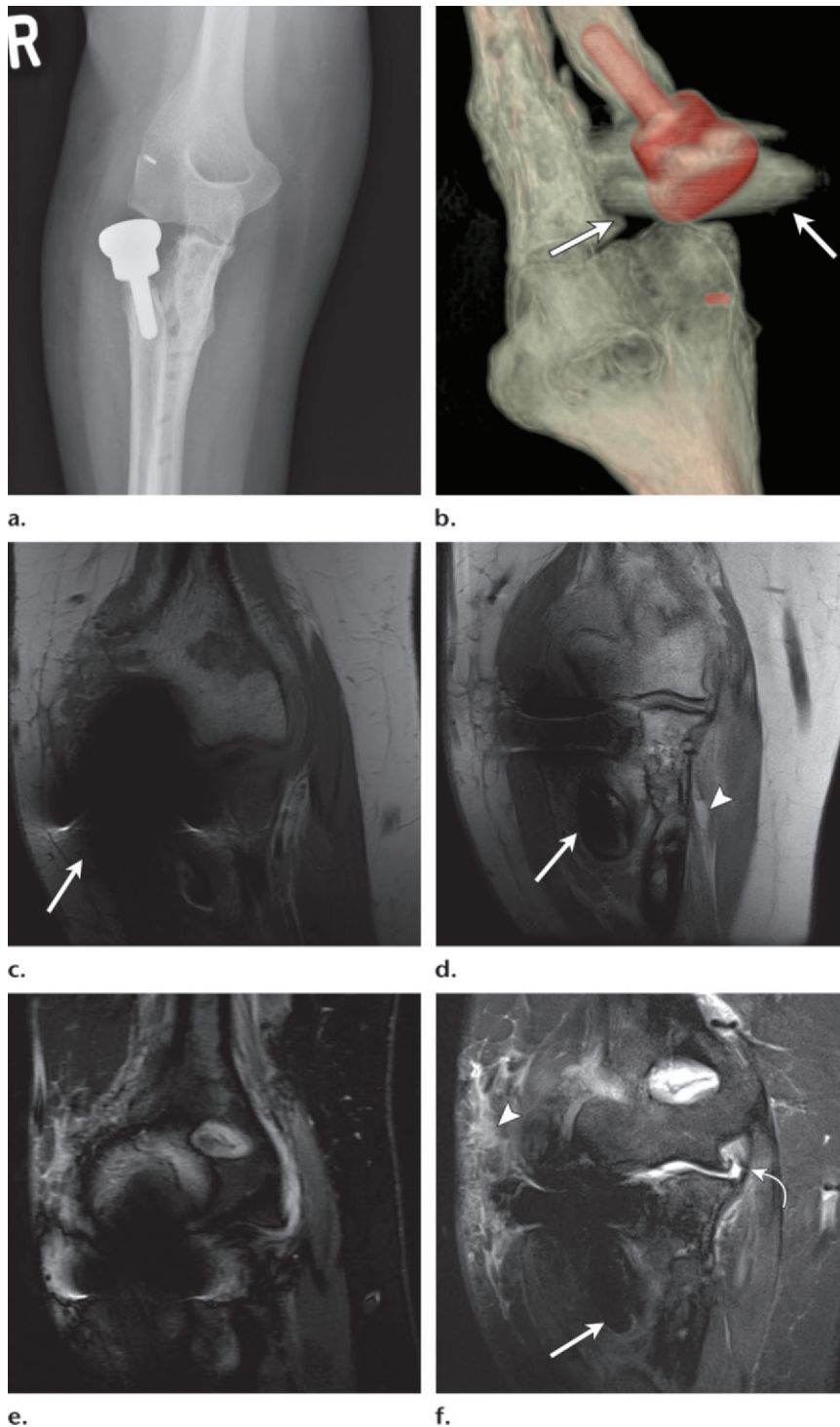


Figure 7. Infection and septic loosening in a 42-year-old woman. The patient's clinical history included substantial right elbow trauma requiring a radial head prosthesis and recent explanation of percutaneous ulnar screws. **(a)** Radiograph shows findings suggestive of loosening and malalignment of the prosthetic head with respect to the capitellum. **(b)** Surface-rendered CT image shows beam-hardening artifact (arrows) that limits detail. **(c)** Coronal proton-density-weighted MR image of the right elbow (without metal suppression) shows marked signal loss artifact (arrow) surrounding the prosthesis. **(d)** Coronal proton-density-weighted WARP MR image reveals high signal intensity at an irregular bone-metal interface (arrow). There is increased detail in the distal part of the postoperative ulna (arrowhead), which shows post-traumatic irregularity and cortical thinning. **(e)** Coronal STIR MR image (without metal suppression) is so laden with signal loss and pileup artifacts that it is nondiagnostic. **(f)** Coronal STIR WARP MR image shows extensive lateral soft-tissue edema (arrowhead), a small effusion (curved arrow), high signal intensity in the ulnar marrow, and a thin rim of high T2 signal intensity at the bone-metal interface of the radial prosthesis (straight arrow). These findings are consistent with infection.

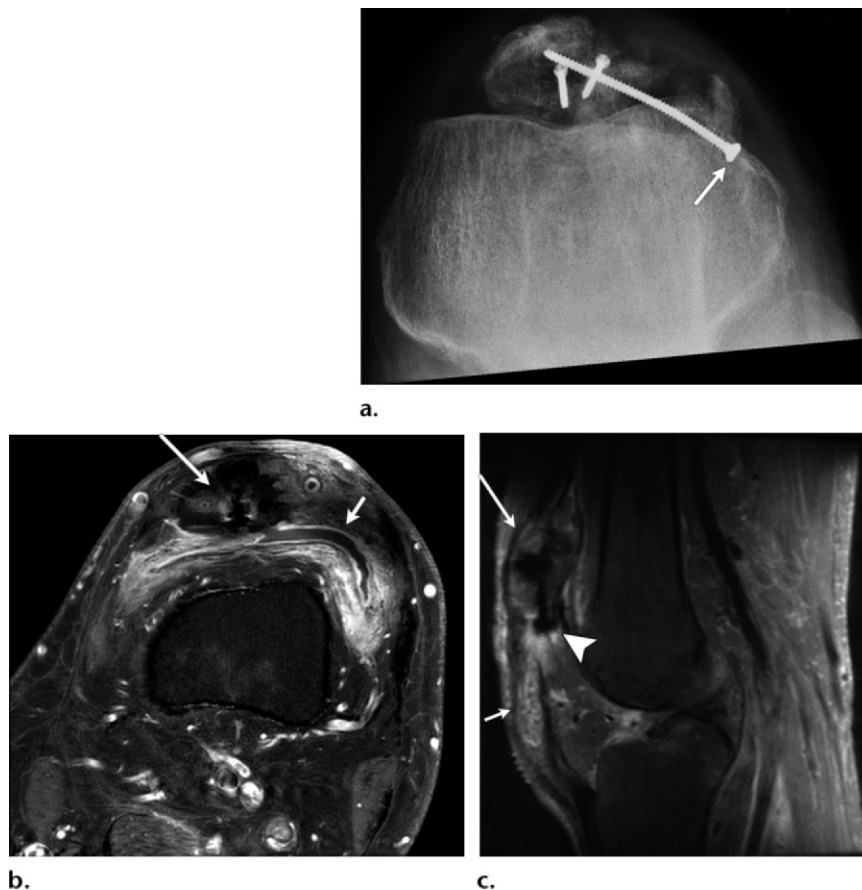


Figure 8. Hardware infection in a 42-year-old man with prior open reduction internal fixation for a left patellar fracture who reported severe knee pain. **(a)** Patellar radiograph shows fragmentation and nonunion of the patellar fracture. The head of the long screw (arrow) is proud relative to the patellar cortex. **(b)** Axial contrast-enhanced fluid-sensitive fat-suppressed MAVRIC MR image shows the fragmented patella (long arrow). Contrast enhancement is seen throughout the synovium and elsewhere (short arrow). **(c)** Sagittal contrast-enhanced fluid-sensitive fat-suppressed MAVRIC MR image shows the irregular patella (long arrow) and the head of the proud screw (arrowhead). Irregular enhancement is seen inferior to the patella and adjacent to a focal area of thickened lamellated synovium (short arrow). The hardware was removed, and tissue and hardware cultures tested positive for *Staphylococcus aureus*.

infection may manifest with nonspecific symptoms and signs, and there can be overlap with pseudotumoral conditions, loosening, and soft-tissue injury (Figs 10, 11).

Loosening

Aseptic loosening can be the result of poor initial fixation, postoperative mechanical disruption of fixation, or biologic failure of fixation secondary to particle disease and osteolysis (33). Although findings of loosening have been described for multiple imaging modalities, prosthetic loosening has largely remained a clinical diagnosis. Although some consider the imaging findings with all modalities to be in large part secondary, there are signs at MR imaging that support the diagnosis of loosening when it is suspected (29,34). The appearance is characterized by a band or line of intermediate-to-high

intraosseous signal intensity that should involve the bone-prosthesis interface. Often, the degree of loosening will lead to trabecular microtrauma and subsequent marrow edema. Early and subtle osteolysis and marrow edema are first identified near the bone-prosthesis interface and may be seen earlier than at radiography (Figs 12, 13).

Tendon Injury

Tendon disruptions or tears and tendinopathy associated with total joint arthroplasty show similar morphology and signal patterns to their non-arthroplasty-associated counterparts. Some common sites of tendon injury include the abductor tendons of the hip, the iliopsoas tendon, and the rotator cuff tendons of the shoulder. One key site of tendinous injury is the myotendinous junction (35). Metal-suppressed MR imaging sequences are a powerful tool for visualizing this region.

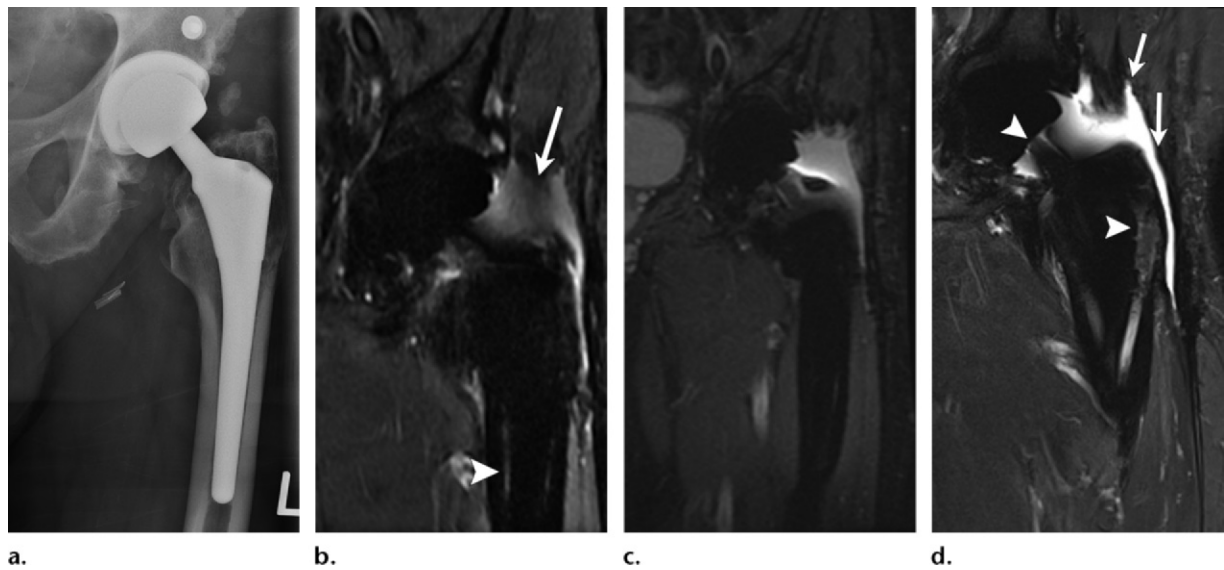


Figure 9. Effusion in a 73-year-old man with a metal-on-metal left hip total arthroplasty device. (a) Radiograph of the left hip does not show signs of acute disease. (b) Coronal STIR MR image (without metal suppression) shows a small effusion (arrow) and a questionable area of high signal intensity at the poorly visualized bone-metal interface (arrowhead). (c) Coronal STIR MARS MR image adds little additional information. (d) Coronal STIR 3.0-T WARP MR image shows the trochanteric bone-metal interface and the prosthetic neck (arrowheads) in robust detail, as well as the junction of the effusion and regional soft tissues (arrows).

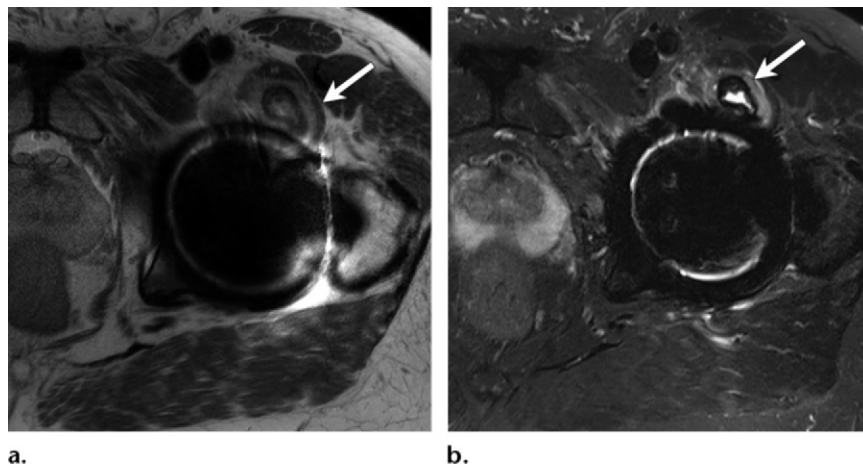


Figure 10. Images in a 66-year-old man with a painful left hip after left hip cobalt-chromium total arthroplasty. Metallosis was suspected clinically because of elevated blood levels of cobalt and chromium. Axial T2-weighted (a) and STIR (b) WARP MR images show an enlarged, bilobed, thick-walled iliopsoas bursa consistent with bursitis (arrow). Aspiration and histologic analysis demonstrated no evidence of ALVAL. This case illustrates that elevated blood chromium and cobalt levels are sensitive but not specific for metallosis.

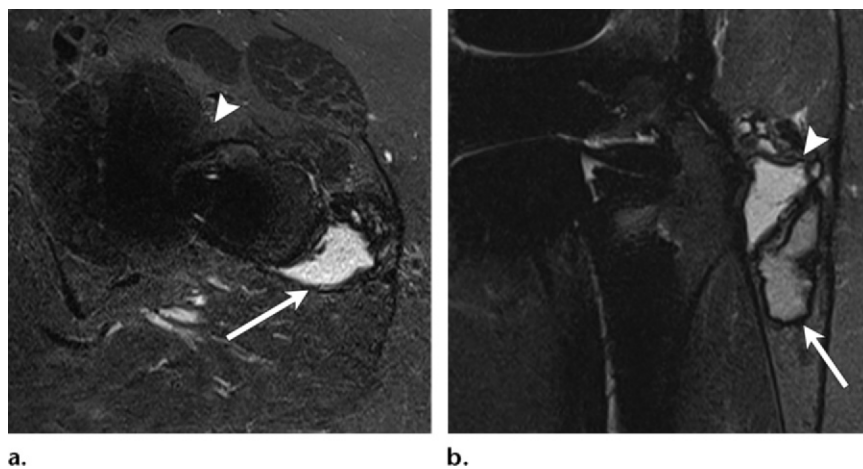
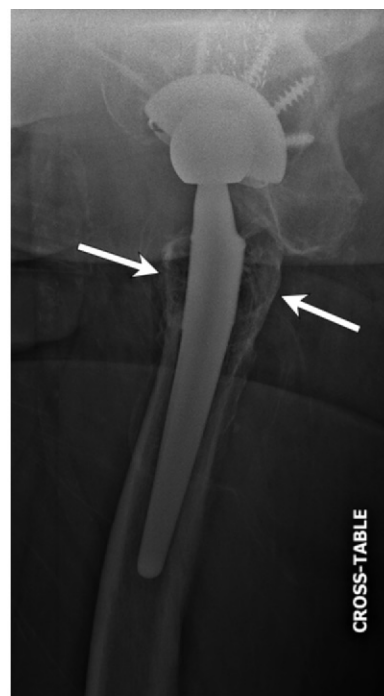
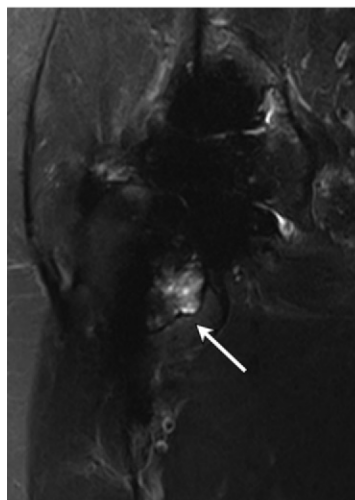


Figure 11. Effusion and pseudotumor in a 72-year-old woman with ongoing left hip pain several years after metal-on-metal total hip arthroplasty (cobalt-chromium alloy). Infection was suspected clinically. (a) Axial STIR MARS MR image shows an irregular fluid collection with high T2 signal intensity (arrow) adjacent to the greater trochanter. Marked through-plane artifact is seen near the acetabular component (arrowhead). (b) Coronal STIR MARS MR image better characterizes the irregular lobulated fluid collection, which has high T2 signal intensity superiorly (arrowhead) and intermediate T2 signal intensity in the inferior lobulation (arrow). Subsequent fluid aspiration demonstrated no evidence of infection.

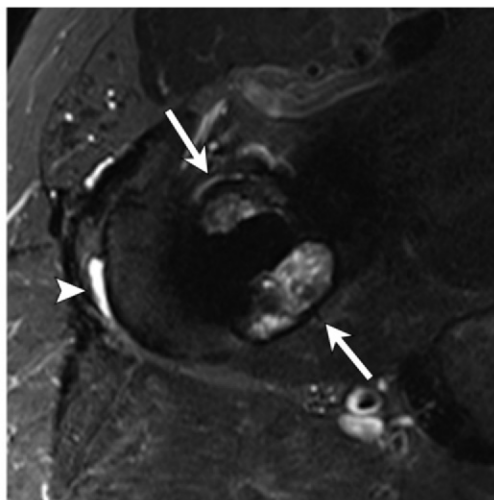
Figure 12. Aseptic loosening in a 69-year-old man with a right hip cobalt-chromium metal-on-metal arthroplasty device who had 2 months of pain. Referring providers suspected trochanteric bursitis or metallosis. (a) Lateral radiograph shows mild osteopenia of the greater and lesser trochanters (arrows), a finding suggestive of stress shielding or osteolysis. (b) Coronal 1.5-T STIR MARS MR image is laden with signal loss artifact, but there is a suspicious area of intermediate-to-high T2 signal intensity in the lesser trochanter (arrow) that is consistent with marrow edema. (c) On an axial 3.0-T STIR WARP MR image, the artifact is greatly reduced, revealing the extent of the marrow abnormality. Intermediate-to-high T2 signal intensity is seen surrounding the prosthetic stem (arrows), a finding consistent with loosening. Note the small effusion (arrowhead) adjacent to the greater trochanter; this effusion was not visible before more advanced metal-suppression techniques were used. Infection was not suspected in this case because of the lack of surrounding high T2 signal intensity in the soft tissues.



a.



b.



c.

Because the myotendinous junction is in close proximity to the arthroplasty components (particularly at the shoulder), care should be taken to ensure that signal abnormalities in this transition zone are not secondary to residual metal artifact.

Muscle Injury

Muscular injury associated with orthopedic implants is often not detectable at radiography. Unlike other cross-sectional modalities such as US and CT, MR imaging can be used to more effectively localize muscular lesions, determine their acuity, infer causality, and characterize associated regional findings (36). Metal suppression plays a key role in depicting pathologic conditions of muscle because unsuppressed metallic artifact

often obscures muscular boundaries and interferes with muscle signal determination. Fortunately, the site of diseased or injured muscle may be somewhat remote from the arthroplasty device itself. This allows diagnostic-quality images to be obtained even if some degree of metal artifact remains after all attempts at suppression have been exhausted. Muscular injury is typified by architectural disruption or distortion, fluid accumulation, and associated tendinous or myotendinous disruption. The length of the muscle strain or tear has been correlated with recovery time, so care should be taken to evaluate not only the degree of architectural disruption but also the overall length of the abnormality compared with that of the entire muscle (37). Hemorrhage can appear as intramus-

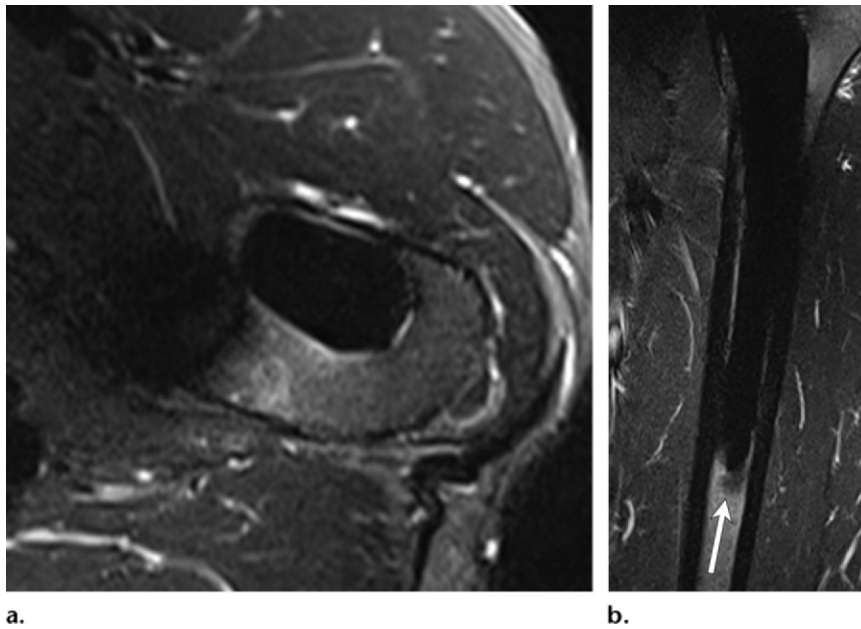


Figure 13. Images in a 62-year-old man with a left hip prosthesis and clinical suspicion for loosening. **(a)** Axial STIR WARP MR image shows a crisp bone-metal interface. There is a minimal degree of pileup and signal loss artifact. **(b)** Coronal STIR WARP MR image shows a similarly discrete bone-metal interface. Low T2 signal intensity is seen at the inferior tip of the prosthetic stem (Gruen zone 4) (arrow). No loosening was identified.

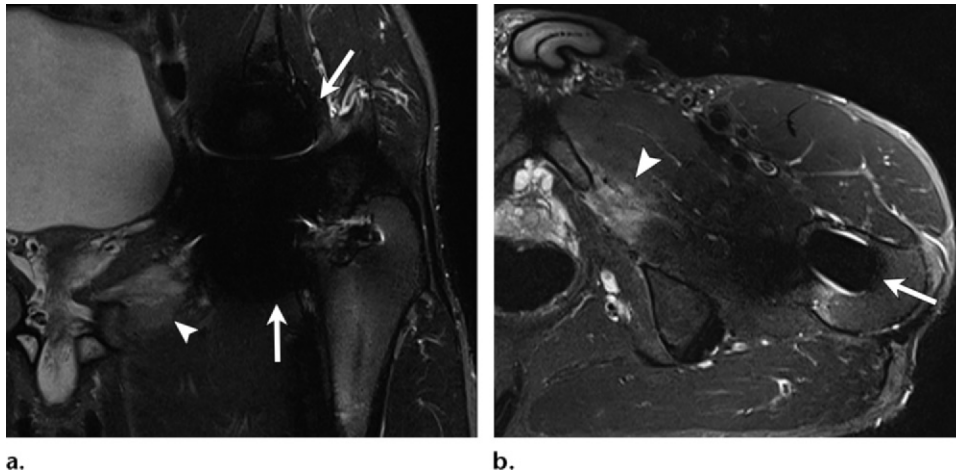


Figure 14. Muscle injury in a 58-year-old man after left hip total arthroplasty. His hip pain had been increasing for 6 weeks. **(a)** Coronal STIR WARP MR image shows high T2 signal intensity in the obturator externus (arrowhead), a finding that suggests muscle injury. The high degree of signal loss artifact around the prosthesis (arrows) limits regional detail. **(b)** Axial STIR WARP MR image shows high T2 signal intensity in the obturator externus muscle fibers (arrowhead), a finding consistent with muscle contusion and areas of muscle tear. The bone-metal interface (arrow) is well delineated, and artifact is greatly reduced. This case illustrates the benefit of imaging in an alternative plane to reduce artifact.

cular blood products or a discrete hematoma. MR imaging signal characteristics of muscular hemorrhage parallel those of hemorrhages elsewhere in the body. One example of muscular injury is illustrated in Figure 14. Postinjury sequelae include retraction and atrophy.

The Special Case of Shoulder Arthroplasty

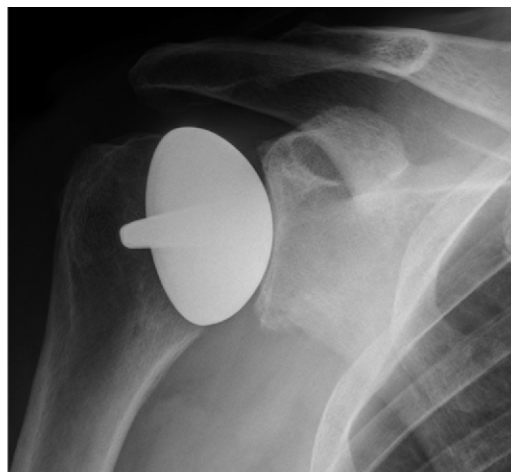
Total shoulder arthroplasty remains a highly problematic area for MR imaging evaluation, even with use of multispectral metal-suppression sequences. The hemispheric geometry of the prosthesis produces complex susceptibility artifacts that are

difficult to control with both basic and advanced methods. Despite the high degree of in-plane and through-plane artifacts at the shoulder, metal-suppression sequences can reveal anatomy and pathologic states that cannot be visualized with conventional imaging (Fig 15). Common causes of failed shoulder arthroplasty include rotator cuff abnormalities, deltoid muscle disease, loosening, and implant component failure (38).

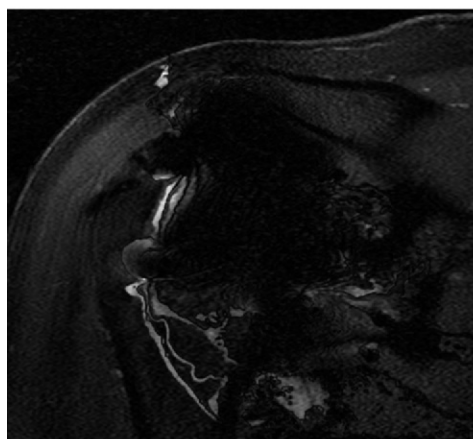
Conclusion

Total joint arthroplasty is an increasingly common orthopedic procedure, and patient age at implantation continues to decrease. MR imaging with

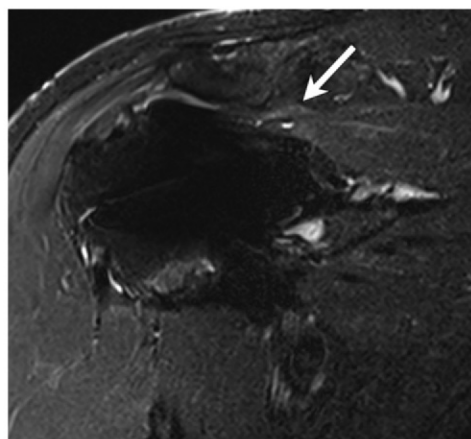
Figure 15. Images in a 66-year-old woman with clinical suspicion for rotator cuff injury after right shoulder hemiarthroplasty. (a) Frontal radiograph shows unremarkable findings. (b) Coronal STIR MR image (without metal suppression) is nondiagnostic because of severe in-plane and through-plane artifacts. (c) Coronal STIR MARS MR image shows reduced in-plane artifact, with improved visibility of the supraspinatus (arrow).



a.



b.



c.

metal-suppression sequences is a powerful tool in detection of arthroplasty-related complications. Radiologists play a key role in optimizing MR imaging sequences to provide diagnostic-quality images, and, with the introduction of advanced multispectral metal-suppression sequences, our role in the diagnosis and treatment of arthroplasty-related complications continues to expand.

Acknowledgments.—Special recognition to Gwen Mack, MFA, Nadezhda Kiriyak, BFA, and Margaret Kowaluk, BS, University of Rochester Medical Center, Rochester, NY, for their professional assistance with the figures, graphics, and image preparation.

References

- Hall MJ, DeFrances CJ, Williams SN, Golosinskiy A, Schwartzman A. National hospital discharge survey: 2007 summary. *Natl Health Stat Rep* 2010;29(29):1–20, 24.
- Ruiz D Jr, Koenig L, Dall TM, et al. The direct and indirect costs to society of treatment for end-stage knee osteoarthritis. *J Bone Joint Surg Am* 2013;95(16):1473–1480.
- Pavarini E, Koch E, Schollwöck U, eds. Emergent phenomena in correlated matter. Vol 3. Jülich, Germany: Forschungszentrum Jülich and Institute for Advanced Simulation, 2013.
- Shokrollahi H. Contrast agents for MRI. *Mater Sci Eng C* 2013;33(8):4485–4497.
- Lee MJ, Kim S, Lee SA, et al. Overcoming artifacts from metallic orthopedic implants at high-field-strength MR imaging and multi-detector CT. *RadioGraphics* 2007;27(3):791–803.
- Butts K, Pauly JM, Gold GE. Reduction of blurring in view angle tilting MRI. *Magn Reson Med* 2005;53(2):418–424.
- Hargreaves BA, Worters PW, Pauly KB, Pauly JM, Koch KM, Gold GE. Metal-induced artifacts in MRI. *AJR Am J Roentgenol* 2011;197(3):547–555.
- Olsen RV, Munk PL, Lee MJ, et al. Metal artifact reduction sequence: early clinical applications. *RadioGraphics* 2000;20(3):699–712.
- Bachschmidt T, Lipps F, Nittka M. Syngo WARP: metal artifact reduction techniques in magnetic resonance imaging. http://www.healthcare.siemens.com/siemens_hwem-hwem_sxxa_websites-context-root/wcm/idc/groups/public/@global/@imaging/@mri/documents/download/mdaw/mzix/~edis/syngo_warp_metal_artifact_reduction_techniques_in_mri-00284426.pdf. Published 2012; accessed October 2014.
- Cho ZH, Kim DJ, Kim YK. Total inhomogeneity correction including chemical shifts and susceptibility by view angle tilting. *Med Phys* 1988;15(1):7–11.
- Lu W, Pauly KB, Gold GE, Pauly JM, Hargreaves BA. SEMAC: slice encoding for metal artifact correction in MRI. *Magn Reson Med* 2009;62(1):66–76.
- den Harder JC, van Yperen GH, Blume UA, Bos C. Off-resonance suppression for multispectral MR imaging near metallic implants. *Magn Reson Med* 2014;73(1):233–243.
- Hayter CL, Koff MF, Shah P, Koch KM, Miller TT, Potter HG. MRI after arthroplasty: comparison of MAVRIC and conventional fast spin-echo techniques. *AJR Am J Roentgenol* 2011;197(3):W405–W411.
- Koff MF, Shah P, Potter HG. Clinical implementation of MRI of joint arthroplasty. *AJR Am J Roentgenol* 2014;203(1):154–161.

15. Koch KM, Brau AC, Chen W, et al. Imaging near metal with a MAVRIC-SEMAC hybrid. *Magn Reson Med* 2011;65(1):71–82.
16. Tayton ER, Smith JO, Evans N, et al. Effects of setting bone cement on tissue-engineered bone graft: a potential barrier to clinical translation? *J Bone Joint Surg Am* 2013;95(8):736–743.
17. Lee YH, Lim D, Kim E, Kim S, Song H-T, Suh J-S. Usefulness of slice encoding for metal artifact correction (SEMAC) for reducing metallic artifacts in 3-T MRI. *Magn Reson Imaging* 2013;31(5):703–706.
18. Robinson E, Henckel J, Sabah S, Satchithananda K, Skinner J, Hart A. Cross-sectional imaging of metal-on-metal hip arthroplasties: can we substitute MARS MRI with CT? *Acta Orthop* 2014;85(6):577–584.
19. Siddiqui IA, Sabah SA, Satchithananda K, et al. A comparison of the diagnostic accuracy of MARS MRI and ultrasound of the painful metal-on-metal hip arthroplasty. *Acta Orthop* 2014;85(4):375–382.
20. Wiley KF, Ding K, Stoner JA, Teague DC, Yousuf KM. Incidence of pseudotumor and acute lymphocytic vasculitis associated lesion (ALVAL) reactions in metal-on-metal hip arthroplasties: a meta-analysis. *J Arthroplasty* 2013;28(7):1238–1245.
21. Hart AJ, Satchithananda K, Liddle AD, et al. Pseudotumors in association with well-functioning metal-on-metal hip prostheses: a case-control study using three-dimensional computed tomography and magnetic resonance imaging. *J Bone Joint Surg Am* 2012;94(4):317–325.
22. Watters TS, Cardona DM, Menon KS, Vinson EN, Bolognesi MP, Dodd LG. Aseptic lymphocyte-dominated vasculitis-associated lesion: a clinicopathologic review of an underrecognized cause of prosthetic failure. *Am J Clin Pathol* 2010;134(6):886–893.
23. Anderson H, Toms AP, Cahir JG, Goodwin RW, Wimhurst J, Nolan JF. Grading the severity of soft tissue changes associated with metal-on-metal hip replacements: reliability of an MR grading system. *Skeletal Radiol* 2011;40(3):303–307.
24. Thomas MS, Wimhurst JA, Nolan JF, Toms AP. Imaging metal-on-metal hip replacements: the Norwich experience. *HSS J* 2013;9(3):247–256.
25. Nawabi DH, Gold S, Lyman S, Fields K, Padgett DE, Potter HG. MRI predicts ALVAL and tissue damage in metal-on-metal hip arthroplasty. *Clin Orthop Relat Res* 2014;472(2):471–481.
26. De Smet K, De Haan R, Calistri A, et al. Metal ion measurement as a diagnostic tool to identify problems with metal-on-metal hip resurfacing. *J Bone Joint Surg Am* 2008;90(suppl 4):202–208.
27. Tower SS. Arthroprosthetic cobaltism: neurological and cardiac manifestations in two patients with metal-on-metal arthroplasty: a case report. *J Bone Joint Surg Am* 2010;92(17):2847–2851.
28. Mayo Clinic Medical Laboratories MCM. Evaluation of metal-on-metal wear of orthopedic implants: the role of serum chromium and cobalt analysis. <http://www.mayomedicallaboratories.com/articles/communique/2012/01.html>. Published 2012. Accessed February 1, 2015.
29. Potter HG, Foo LF, Nestor BJ. What is the role of magnetic resonance imaging in the evaluation of total hip arthroplasty? *HSS J* 2005;1(1):89–93.
30. Athanasou NA, Quinn J, Bulstrode CJ. Resorption of bone by inflammatory cells derived from the joint capsule of hip arthroplasties. *J Bone Joint Surg Br* 1992;74(1):57–62.
31. Cooper HJ, Ranawat AS, Potter HG, Foo LF, Koob TW, Ranawat CS. Early reactive synovitis and osteolysis after total hip arthroplasty. *Clin Orthop Relat Res* 2010;468(12):3278–3285.
32. Malinzak RA, Ritter MA, Berend ME, Meding JB, Olberding EM, Davis KE. Morbidly obese, diabetic, younger, and unilateral joint arthroplasty patients have elevated total joint arthroplasty infection rates. *J Arthroplasty* 2009;24(6 suppl):84–88.
33. Abu-Amer Y, Darwech I, Clohisey JC. Aseptic loosening of total joint replacements: mechanisms underlying osteolysis and potential therapies. *Arthritis Res Ther* 2007;9(1 suppl 1):S6.
34. Temmerman OP, Raijmakers PG, Berkhof J, Hoekstra OS, Teule GJ, Heyligers IC. Accuracy of diagnostic imaging techniques in the diagnosis of aseptic loosening of the femoral component of a hip prosthesis: a meta-analysis. *J Bone Joint Surg Br* 2005;87(6):781–785.
35. Taneja AK, Kattapuram SV, Chang CY, Simeone FJ, Bredella MA, Torriani M. MRI findings of rotator cuff myotendinous junction injury. *AJR Am J Roentgenol* 2014;203(2):406–411.
36. May DA, Disler DG, Jones EA, Balkissoon AA, Manaster BJ. Abnormal signal intensity in skeletal muscle at MR imaging: patterns, pearls, and pitfalls. *RadioGraphics* 2000;20(Spec No):S295–S315.
37. Connell DA, Schneider-Kolsky ME, Hoving JL, et al. Longitudinal study comparing sonographic and MRI assessments of acute and healing hamstring injuries. *AJR Am J Roentgenol* 2004;183(4):975–984.
38. Nwawka OK, Konin GP, Sneag DB, Gulotta LV, Potter HG. Magnetic resonance imaging of shoulder arthroplasty: review article. *HSS J* 2014;10(3):213–224.